HHS Public Access

Author manuscript

Mol Psychiatry. Author manuscript; available in PMC 2022 December 01.

Published in final edited form as:

Mol Psychiatry. 2022 August ; 27(8): 3520–3531. doi:10.1038/s41380-021-01174-2.

Atypical perineuronal nets in the CA2 region interfere with social memory in a mouse model of social dysfunction

Elise C. Cope, PhD,

Anna D. Zych, MS,

Nicole J. Katchur, BA,

Renée C. Waters, BA,

Blake J. Laham, MA,

Emma J. Diethorn, BA,

Christin Y. Park, BA,

William R. Meara, BS,

Elizabeth Gould, PhD*

Princeton Neuroscience Institute, Princeton University, Princeton, NJ 08544

Abstract

Social memory dysfunction is an especially devastating symptom of many neuropsychiatric disorders, which makes understanding the cellular and molecular processes that contribute to such abnormalities important. Evidence suggests that the hippocampus, particularly the CA2 region, plays an important role in social memory. We sought to identify potential mechanisms of social memory dysfunction in the hippocampus by investigating features of neurons, glia, and the extracellular matrix (ECM) of BTBR mice, an inbred mouse strain with deficient social memory. The CA2 is known to receive inputs from dentate gyrus adult-born granule cells (abGCs), neurons known to participate in social memory, so we examined this cell population and found fewer abGCs, as well as fewer axons from abGCs in the CA2 of BTBR mice compared to controls. We also found that BTBR mice had fewer pyramidal cell dendritic spines, in addition to fewer microglia and astrocytes, in the CA2 compared to controls. Along with diminished neuronal and glial elements, we found atypical perineuronal nets (PNNs), specialized ECM structures that regulate plasticity, in the CA2 of BTBR mice. By diminishing PNNs in the CA2 of BTBR mice to control levels, we observed a partial restoration of social memory. Our findings suggest that the CA2 region of BTBR mice exhibits multiple cellular and extracellular abnormalities and identify atypical PNNs as one mechanism producing social memory dysfunction, although the contribution of reduced abGC afferents, pyramidal cell dendritic spine and glial cell numbers remains unexplored.

*To whom correspondence should be addressed: Elizabeth Gould PhD, Princeton Neuroscience Institute, Washington Rd, Princeton University, Princeton NJ 08544, goulde@princeton.edu.

Conflicts of Interest

Authors declare that they have no conflict of interest.

Introduction

Social memory is an essential function that forms the basis of adaptive social interactions, including between family members and within groups of unrelated individuals. Social memory dysfunction is a feature of many neuropsychiatric illnesses, such as autism spectrum disorder (ASD), schizophrenia, major depressive disorder, and Alzheimer's disease [1,2] and is considered to be a particularly devastating symptom in terms of its effects on overall function and quality of life [3,4]. Studies have sought to determine the neural mechanisms of social memory using rodent models, and many of these reports have provided evidence that the hippocampus plays an important role in this capability [5,6]. Involvement of this brain region is perhaps not surprising given that human conditions with social memory impairments often exhibit hippocampal abnormalities [7–9].

Studies in mice have shown that social memory requires the CA2 region of the hippocampus. Chemogenetic and optogenetic inactivation of the CA2 and lesions of the CA2 have been shown to selectively impair social recognition memory, while optogenetic activation of CA2 neurons has been show to improve social recognition memory, suggesting that this region is critical for social memory formation [10–13]. Several studies have shown that the dentate gyrus is important for social memory and in particular, dentate gyrus granule cells that are born in adulthood appear to be essential for storing and/or retrieving social memories [14–18]. Since adult-born granule cells (abGCs) in the dentate gyrus are known to project to the CA2 [19], it seems likely that they exert their influence over social memory through this circuit.

In the adult mammalian brain, perineuronal nets (PNNs), specialized extracellular matrix (ECM) lattice-like structures that surround neurons, have been shown to promote synaptic stabilization [20–22]. In the hippocampus, PNNs typically form around inhibitory interneurons [23], but in the CA2 region, PNNs have been observed surrounding both inhibitory and excitatory neurons [24–25]. A recent study suggests that PNNs surrounding pyramidal neurons in the CA2 represent those ensheathing the terminals of inhibitory synapses projecting onto these cells [25]. PNNs in the CA2 have been shown to inhibit synaptic plasticity [24], but their potential role in behaviors linked to the CA2 remains relatively unexplored. Along these lines, it is interesting to note that irregularities in PNNs have been observed as a feature shared across neuropsychiatric disorders that are associated with social behavior dysfunction [21,22,26]. In order to investigate potential mechanisms of social memory impairments, we examined an inbred strain of social dysfunction, BTBR *T+ Itpr3tf*/J (BTBR) mice [27,28], for evidence of abnormalities in neuronal structure and circuitry as well as in PNNs in the CA2 region. Because microglia and astrocytes also influence synaptic signaling [29–31] and have been linked to social memory [32], we investigated these nonneuronal cells for potential abnormalities as well. We found that social memory dysfunction in BTBR mice is accompanied by aberrations in pyramidal cell dendritic spines, afferents from the abGCs of the dentate gyrus, microglia and astrocytes in the CA2 region. We also observed abnormal PNNs in the CA2 of BTBR mice and found that reducing PNNs to control levels partially restored social memory in this mouse model of social dysfunction.

Materials and Methods

Animals

Age-matched adult male C57BL/6J and BTBR *T+ Itpr3tf*/J (BTBR) mice were obtained from The Jackson Laboratory and group-housed on a reverse 12 h light/dark cycle. See Supplementary Methods.

Behavioral testing

Mice underwent testing in the following order: 3-chamber social test, object location memory, direct social interaction test. For PNN degradation experiments, mice were only tested on the direct social interaction test. Sociability and social novelty recognition were assessed with a 3-chamber box [10, 28] over a 2-day period. To assess social memory, 3 versions of the direct social interaction test were adapted from established protocols [10, 12, 18]. See Supplementary Methods.

Histology

Mice were perfused and hippocampal sections were stained with *Wisteria floribunda* agglutinin (WFA) lectin or antibodies for 3R-Tau, Purkinje cell protein 4 (PCP4), mCherry, parvalbumin (PV), orthodenticle homeobox 2 (OTX2), ionized calcium binding adaptor molecule 1 (iba1), glial fibrillary acidic protein (GFAP), or aggrecan. See Supplementary Methods, Supplementary Table 1. Diolistic labeling of CA2 pyramidal neurons with the fluorescent carbocyanine dye DiI (Sigma-Aldrich) was achieved using a Helios Gene Gun System (BioRad) as previously described [33].

Histological analyses

Z-stack images of the dentate gyrus (DG), CA3, CA2, and CA1 regions of the hippocampus, as well as of the choroid plexus, were obtained with a Zeiss confocal microscope (LSM 700). See Supplementary Methods. Volume, cell density, optical intensity, and dendritic spine density measurements were made using Image J software or Stereo investigator software (MBF Bioscience).

Surgical procedures

To label granule cells projecting to the CA2, unilateral injections of the retrograde virus rAAV-EF1a-mCherry-WPRE-hGHpA virus (AAV2-retro, made by the Princeton Viral Core, titer: 1×10^{13}) were made in the CA2. To explore whether CA2 PNNs participate in social memory, bilateral injections of chondroitinase ABC (chABC, 50 U/ml, Sigma), an enzyme that temporarily degrades PNNs by digesting the sulfated sugar chains responsible for PNN glycoprotein function, or the control enzyme penicillinase (PNase, 50 U/ml, Sigma) were made in the CA2. CA2 coordinates were −1.82 AP, +/−2.15 ML, and −1.7 DV for control mice and −1.7 AP, +/−2.6 ML, and −1.4 DV for BTBR mice. See Supplementary Methods.

Statistical analyses

Data were analyzed with a linear mixed-effects model, unpaired two tailed student's t-test, Mann-Whitney U tests or 2-way ANOVA and repeated measures 2 or 3-way ANOVA with Bonferroni post hoc comparisons. See Supplementary Methods.

Results

BTBR mice have impaired social and object memory

Consistent with previous reports [28, 34], we found that BTBR mice had impaired sociability in the 3-chamber test. While control mice preferred the social stimulus over the novel object, BTBR showed no such preference (Figure 1A). We then examined social novelty recognition 24 hours later. Control mice had a strong preference for a novel mouse, while BTBR mice spent similar amounts of time investigating a familiar mouse and a novel mouse (Figure 1B), suggesting an impairment in their ability to recognize a familiar conspecific. We corroborated this finding using the direct social interaction test [10, 12, 18] with a 1-hour delay between presentation of a novel mouse and re-exposure to the same mouse. BTBR mice investigated novel mice less than controls. In addition, BTBR mice showed no difference in investigation times between novel and familiar mice (Figure 1C). Both control and BTBR mice investigation times did not decrease during the second encounter when a new, novel mouse was introduced (Figure 1D), indicating that sociability was not reduced from repeated social interactions.

The hippocampus is well known for its other cognitive functions including processing information related to context and spatial location [35]. Consistent with previous findings [36], we found that BTBR mice have impairments in hippocampus-dependent object location memory as demonstrated by their low discrimination ratios compared to controls (Supplementary Figure 1).

BTBR mice have fewer axons from abGCs in the CA2 than controls

Diminished adult neurogenesis has been shown to impair social memory performance in mice [14–18]. Granule cells of the DG, including abGCs, project to the CA2 [19, 37]. Since the CA2 has been linked to social memory [10–12], we examined its afferents from the DG. We first used 3R-Tau to label abGCs and their mossy fiber axons [19] (Figure 2A). Consistent with previous reports [38], we found decreases in the density of 3R-Tau+ cell bodies in the dorsal DG (Figure 2B) and ventral DG (Control: 19158±2049 cells per mm^3, BTBR: 9991±1729 cells per mm^3, $t_{16} = 3.42$, $p = 0.0035$) of BTBR mice compared to controls. Examination of 3R-Tau+ fibers revealed BTBR mice have considerably fewer abGC mossy fibers in the CA2 compared to controls (Figure 2C).

To examine the overall population of granule cells that projects to the CA2, we injected a retrograde recombinant AAV (AAV2-retro) into the CA2. In addition to cell body uptake at the site of injection, AAV2-retro enters through the terminals of axons and is transported retrogradely toward the cell body of origin [39]. Two weeks after virus injection, mCherry+ cells were identified in the CA2 and DG of both control and BTBR mice, with similar virus expression and cell morphology observed in both strains (Figure 2D,E). Many of

the mCherry+ granule cells were primarily located in the superficial layer of the granule cell layer (Figure 2E), suggesting typical input to CA2 from mature granule cells in BTBR mice. Taken together, these findings suggest that in BTBR mice, the pathway from developmentally generated DG granule cells to the CA2 seems similar to controls. However, the number of abGCs and their projections to the CA2 is substantially lower.

BTBR mice have a smaller CA2 region, with fewer pyramidal cell dendritic spines, microglia, and astrocytes, compared to controls

To determine whether CA2 structure was different in BTBR mice, we used the CA2 marker PCP4 in comparison with controls [40, 41] and found a significantly smaller CA2 volume in BTBR mice (Figure 3A). We then explored whether BTBR mice had different numbers of dendritic spines on CA2 pyramidal neurons using DiI-labeling and found lower dendritic spine density on both apical and basal dendrites compared to controls (Figure 3B). Since glia are known to regulate synaptic numbers in the healthy and diseased brain [42–45], we investigated whether there were changes in the number of microglia and astrocytes in BTBR mice. We found fewer iba1+ microglia (Figure 3C) and GFAP+ astrocytes (Figure 3D) in the CA2 of BTBR mice compared to controls.

PNNs and OTX2 are atypical in the CA2 of BTBR mice compared to controls

PNNs are specialized ECM structures that surround some neurons and regulate plasticity [21, 22]. Consistent with previous work [24–25], using the lectin-based stain WFA, we found intense staining surrounding both pyramidal cells and inhibitory interneurons in the CA2 of controls. Compared to controls, BTBR mice had an increase in WFA+ volume in the CA2 (Figure 4A). WFA staining intensity was also notably increased in the CA2 of BTBR mice (Figure 4B). Examination of individual 2μm optical sections revealed that the WFA staining was clearly perineuronal, surrounding PCP4-labeled cell bodies in the pyramidal cell layer (Supplementary Figure 2). To explore this difference further, we investigated the expression of aggrecan, a proteoglycan that is common to most, if not all PNNs, and found no differences in aggrecan volume (Control: .00237 ± .00013 mm^3, BTBR: .00227±.00012 mm^3, $t_{14} = 0.5360$, $p = 0.9095$). Since WFA is thought to recognize only those PNNs that have specific sulfation patterns, these findings together suggest that the number of CA2 cells with PNNs may be similar between BTBR and control mice, but that PNN composition is different. We next investigated the transcription factor OTX2 because of its association with the formation of PNNs in the developing visual cortex [46] and found differences in the CA2 that were consistent with our WFA data; BTBR mice exhibited greater OTX2 intensity in the CA2 compared to controls (Supplementary Figure 3B). Since OTX2 is synthesized in the choroid plexus in adulthood and then distributed throughout the brain where it is taken up by certain neurons [47], we next examined the choroid plexus and found that compared to controls, BTBR mice had decreased OTX2 intensity (Supplementary Figure 3A).

PNNs are atypical in additional subregions within the hippocampus of BTBR mice compared to controls.

We examined WFA+ cell numbers and staining intensity in other subregions within the hippocampus. In BTBR mice, we found a decrease in the number of WFA+ cells in both the dorsal and ventral DG (Supplementary Figure 4). These decreases were specific to WFA+

cells that colocalized with PV (Supplementary Figure 4). BTBR mice also had fewer PV+ cells in the DG (Supplementary Figure 4). Compared to controls, there was no difference in WFA mean intensity in the DG of BTBR mice regardless of whether WFA+ PNNs colocalized with PV (Supplementary Figure 4). In the dorsal CA3 (dCA3) and ventral CA3 (vCA3) of BTBR mice, there was an increase in the number of WFA+ cells that did not co-label with PV (Supplementary Figure 5). No differences were detected in the number of WFA+ cells that colocalized with PV or in the number of PV+ cells in the dCA3 or vCA3 of BTBR mice (Supplementary Figure 5). In the dCA3, BTBR mice had reduced WFA mean intensity of WFA+ cells that colocalized with PV but not in WFA+ cells that did not colocalize with PV (Supplementary Figure 5). There was no change in WFA staining intensity of PV+ or PV- cells in the vCA3 of BTBR mice compared to controls (Supplementary Figure 5). In the dorsal CA1 of BTBR mice, there was no difference in the number or intensity of WFA cells regardless of whether they were co-labeled with PV in BTBR mice compared to controls (Supplementary Figure 6). We next analyzed PNNs in the ventral CA1 (vCA1), a hippocampal subregion that has also been associated with social memory [13]. In the vCA1 of BTBR mice, however, there was no difference in WFA cell numbers regardless of whether they were co-labeled with inhibitory interneuron marker PV (Figure 5C). We then analyzed WFA staining intensity of individual WFA+ PNNs. There was no difference in WFA staining intensity of PV+ or PV- cells in BTBR mice compared to controls (Figure 5D).

Reducing CA2 PNNs in control mice impairs social memory

To explore the involvement of CA2 PNNs in social memory, we first investigated whether degradation of PNNs in the CA2 of control mice would impair social memory performance. Adult mice received bilateral injections of either chABC, an enzyme known to digest sulfated sugar chains on the glycoproteins that form the basis of PNNs [24, 25], or a control enzyme, PNase, into the CA2. Since PNN degradation is temporary after chABC injection, we tested behavior using a 3-trial direct social interaction test paradigm (Figure 5A,B) at 5 days post-injection (DPI), a time when mice had recovered from surgery but WFA+ PNNs have not completely recovered. Control mice injected with PNase had normal social memory, showing decreased interactions with familiar mice, whereas mice injected with chABC spent similar times interacting with novel and familiar mice (Figure 5C). Neither group showed significant increases in interaction times with a new, novel mouse after the familiarization period, although control mice showed a nonsignificant increase (Figure 5D). chABC treatment affected sociability as there was a slight decrease in social investigation times compared to PNase in the first novel trial (Figure 5C).

Reducing PNNs to control levels in BTBR mice improves social memory

We next explored the possibility that atypical PNNs in BTBR mice contribute to their social memory deficit. In pilot studies, we found that WFA staining intensity has been restored to control levels in BTBR mice and is no longer significantly diminished in control mice by 10 DPI of chABC (Supplementary Figure 7). We then examined social memory in control and BTBR mice 10 DPI of PNase or chABC (Figure 5A,B). Control mice injected with PNase or chABC with 10 DPI recovery had normal social memory, showing decreased interaction times toward familiar mice and increased interaction times for novel mice (Figure 5F-H). As

expected given our studies in unoperated BTBR mice, BTBR mice injected with PNase did not show evidence of recognizing familiar mice. However, BTBR mice injected with chABC with a 10 DPI recovery l time displayed some evidence of social memory in that they had decreased interaction times for familiar mice and increased interaction times for novel mice (Figure 5F-H). Consistent with our previous findings, BTBR mice displayed lower levels of sociability in the novel 1 trial compared to control mice. chABC-induced restoration of control-like PNN staining had no restorative effect on sociability as there was no difference in social investigation times between BTBR mice injected with PNase or chABC in the novel 1 trial.

Discussion

Our data indicate that BTBR mice exhibit social memory impairments, as well as multiple cellular and extracellular abnormalities in the CA2, including in measures associated with plasticity, such as abGC afferents, dendritic spines, microglia, astrocytes and PNNs. Synaptic function can be influenced by each of these measures [29, 31] raising multiple possible mechanisms underlying social memory dysfunction in this mouse model. We directly investigated whether atypical PNNs in the CA2 were responsible for social memory impairments in BTBR mice and found that reducing PNNs to control values partially rescued social recognition memory.

CA2 PNNs and social memory

In addition to its unique molecular signature among other hippocampal subregions [48–50], the CA2 is known for its unusually high concentration of PNNs [24]. In other parts of the hippocampus, PNNs surround subsets of inhibitory interneurons, whereas in the CA2, they also surround pyramidal neurons [24, 25]. In the CA2, PNNs have been shown to reduce excitation [24, 51] and facilitate a form of synaptic plasticity associated with social memory, LTD at inhibitory synapses [25]. It has also been suggested that CA2 PNN development during postnatal life is required for the emergence of mature social memory capabilities, and consistent with our findings in adult control mice, degradation of CA2 PNNs has been shown to interfere with social recognition memory [25]. In addition, degradation of PNNs in the entire dorsal hippocampus has been shown to diminish nonsocial hippocampus-dependent memories [52], raising the possibility of a general mechanism linking PNNs to experience-dependent plasticity in the adult hippocampus.

We found that the typically high concentration of PNNs in the CA2 of control mice is further increased in BTBR mice with substantially greater volume and intensity of WFA staining. While this staining intensity was much greater in BTBR mice raising the possibility that it represents diffuse ECM labeling, examination of thin (2μm thick) optical sections revealed that WFA staining was clearly perineuronal, but considerably more intense. Increased WFA staining is consistent with our finding of increased expression of OTX2, a transcription factor known to increase PNNs during development [53], in the BTBR CA2. PNNs comprise chondroitin sulfate proteoglycans (CSPG) with their function determined by both the CSPG composition as well as CSPG sulfation pattern. 4-sulfation, which has been causally linked with substantially reduced plasticity, is the dominant PNN sulfation pattern in older mice

[54, 55]. WFA is not a pan-PNN marker but instead may label PNNs with a 4-sulfation pattern [56]. Aggrecan, on the other hand, is a CSPG thought to be a component of most, if not all, PNNs [56]. Our results of greater WFA labeling without similar changes in aggrecan in the BTBR CA2 suggest that PNNs may not necessarily be increased, but instead, changed in their sulfation patterns such that the plasticity-diminishing 4-sulfation pattern dominates. Thus, our finding that excessive WFA labeling in the CA2 co-occurs with a complete lack of behavioral evidence of social memory is consistent with the interpretation that BTBR mice have a much greater proportion of PNNs with plasticity-inhibiting PNNs. chABC works by digesting sulfated sugar chains on CSPGs, thus eliminating WFA staining temporarily. CSPG sulfated sugar chains typically reconstitute themselves within a few weeks of their degradation. Using a post-chABC survival time when BTBR mice have not yet reached their excessively high WFA labeling seen at baseline but instead, had achieved control-like WFA staining patterns, we found partially rescued social memory. These findings suggest that excessive WFA labeling in the CA2 is causally linked to impaired social experience-dependent plasticity. Since sociability is known to be low in BTBR mice compared to controls [28, 34], this raises the possibility that PNN degradation restored social memory by increasing sociability, however, we found no change in social investigation times in response to novel mouse exposure despite newfound evidence for social recognition suggesting that typical social behavior is only partially rescued in BTBR mice with diminished CA2 PNNs.

Given the evidence suggesting that PNNs facilitate plasticity and social memory in the CA2 [25], our results showing that reduced PNNs coincide with enhanced social memory may seem paradoxical. However, studies in mouse models of Alzheimer's disease and age-related cognitive dysfunction have shown that degradation of PNNs in the perirhinal cortex improves cognitive function on object memory tasks [55,57], suggesting that under certain conditions PNNs may induce a pathological suppression of plasticity and function. Although the exact mechanisms whereby abnormal PNNs may inhibit function remain unknown, some evidence suggests that under control conditions PNNs inhibit LTP at excitatory synapses [24] and since LTP has been shown to be sensitive to vasopressin [58], a neuropeptide in the CA2 important for social memory [12], further suppression by the presence of atypical PNNs may interfere with normal synaptic function in the area. This possibility is consistent with recent findings that abnormal PNNs in the CA2 coincide with a premature developmental downregulation of synaptic plasticity in a MECP2 deletion model [59]. PNNs have also been shown to diminish sharp wave ripples [60], neuronal oscillatory events that play key roles in hippocampal replay underlying memory consolidation [61], presenting an additional mechanism whereby atypical PNNs might adversely affect social memory.

Potential contribution of other hippocampal abnormalities to BTBR social memory dysfunction

The CA2 has been described as a "critical hub" for processing social information [10], but social memory clearly requires other brain regions as well. Within the hippocampus, the CA2 receives inputs from the DG [37] and has connections with the CA1 and CA3 [48]. Since reducing CA2 PNNs to control-like levels in BTBR mice only partially restored social memory function, other abnormalities we detected, including those in PNNs in the DG and CA3, might contribute to dysfunction. The extent to which PNN differences in these areas

contribute to social memory dysfunction remains unexplored. However, it is relevant to note that no PNN differences were detected in the vCA1, a CA2 target known to participate in social memory [13, 62], suggesting that PNN abnormalities are not a ubiquitous feature of the BTBR social memory circuitry.

We identified additional cellular abnormalities in the BTBR CA2 that might contribute to social memory dysfunction. First, afferents from abGCs of the DG are substantially lower in BTBR mice compared to controls, despite apparently normal inputs from mature granule cells. Since abGCs have been linked to social memory [14–18], they may exert this influence through connections with the CA2. Taken together with the reduced dendritic spine density on CA2 pyramidal cells, overall synaptic activity may be diminished to the point of impaired function. We also found lower numbers of microglia and astrocytes in the CA2 of BTBR mice compared to controls. Since both microglia and astrocytes contribute to synaptic function [29–31] and some evidence has shown that hippocampal-specific reductions in microglia causes impaired social memory in mice [32], it raises the possibility that low numbers of glial cells additionally contribute to suboptimal function in BTBR mice. Previous studies examining the hippocampus of BTBR and control mice have identified numerous differences in gene expression, including in genes related to microglia and neuronal growth and maintenance [63,64]. Taken together with the findings of the present study, there are likely multiple, perhaps interrelated, causal factors for producing a deficit of social memory dysfunction.

Potential interactions among PNNs, abGCs, dendritic spines, and glia

BTBR mice are an inbred strain that has been studied extensively because of its well-known deficits in social function [28, 34]. Our findings add to the list of known neuroanatomical abnormalities in this mouse model [65] by showing fewer abGC afferents to the CA2 as well as fewer dendritic spines on CA2 pyramidal cells of BTBR mice compared to controls. Taken together with our observations of differences in PNNs, microglia, and astrocytes in the BTBR CA2 compared to controls, these findings raise questions about whether specific abnormalities are responsible for others. For example, it is possible that lower levels of excitation in the CA2, reflected by sparse excitatory abGC afferents and pyramidal cell dendritic spines, are responsible for atypical PNN formation in the region. Along these lines, a previous study showed that chemogenetic decreases in CA2 neuronal activity increase PNN expression in the CA2 of controls [59]. PNN aberrations themselves may further exaggerate disruptions in neural activity in hippocampal circuits by limiting synaptic plasticity and neuronal oscillations, producing a feedforward loop whereby reduced activity induces PNN abnormalities, which themselves insure the persistence of reduced activity [21, 22].

It is also possible that low numbers of glial cells in the CA2 contribute to abnormal PNNs. Studies have suggested that glia may act as homeostatic regulators of the ECM. For example, microglia have been shown to release proteases that degrade the ECM under conditions of inflammation [66, 67] and across the diurnal rhythm [68]. Microglia-mediated engulfment of the ECM has recently been shown to be important for synaptic plasticity in response to experience [69]. It is possible that social memory function in BTBR mice

is inhibited by the inability of low numbers of microglia to remodel the ECM and allow new synaptic connections to form. It is also worth noting that BTBR mice exhibit white matter abnormalities, including diminished or absent commissural connections [70,71]. These differences are likely related to altered expression of genes associated with axon guidance [70] as well as myelin basic protein in BTBR mice [71]. BTBR mice have also been shown to have altered expression of ECM-related proteins [72], and additional studies have shown that ECM proteins can inhibit both axon outgrowth [73] and myelination [74], raising additional putative connections among BTBR brain abnormalities. These possibilities should be the focus of future work.

Conclusions

Our work suggests that atypical PNNs in the CA2 are at least partially responsible for social memory dysfunction in BTBR mice. These findings may be relevant to neuropsychiatric conditions associated with social memory dysfunction and abnormal expression of PNNs such as ASD, schizophrenia, major depressive disorder, and Alzheimer's disease [1, 2, 21, 22]. Restoring PNNs to normal levels may be a potential therapeutic target for these disorders. Future work is needed to explore the extent to which hippocampal abnormalities in adult neurogenesis and glia also contribute to social memory impairments in BTBR mice.

Supplementary Material

Refer to Web version on PubMed Central for supplementary material.

Acknowledgments

This work was supported by the National Institutes of Health, NIMH 1R01 MH118631–01 to E.G and NIH Training Fellowship T32MH065214 to E.C.C. The authors thank Biorender for assistance with the figure schematics, Sahana Murthy and Brandy A. Briones for helpful comments on the project, and Carla G. Dias, Kristen A. Pagliai, and Amelia Windorski for assistance with histological analyses.

References

1). Williams DL, Goldstein G, Minshew NJ Impaired memory for faces and social scenes in autism: clinical implications of memory dysfunction. Arch Clin Neuropsychol 2005; 20:1–15. [PubMed: 15620811]

2). Porcelli S et al. Social brain, social dysfunction and social withdrawal. Neurosci Biobehav Rev. 2019; 97:10–33. [PubMed: 30244163]

3). Kurtz MM, Bronfeld M, Rose J. Cognitive and social cognitive predictors of change in objective versus subjective quality-of-life in rehabilitation for schizophrenia. Psychiatry Res. 2012; 200:102–107. [PubMed: 22769048]

4). García-Casal JA, Goñi-Imizcoz M, Perea-Bartolomé MV, Soto-Pérez F, Smith SJ, Calvo-Simal S, Franco-Martín M. The efficacy of emotion recognition rehabilitation for people with Alzheimer's Disease. J Alzheimers Dis. 2017;57:937–951. [PubMed: 28304290]

5). Kogan JH, Frankland PW, Silva AJ. Long-term memory underlying hippocampus-dependent social recognition in mice. Hippocampus. 2000; 10:47–56. [PubMed: 10706216]

6). Montagrin A, Saiote C, Schiller D. The social hippocampus. Hippocampus. 2018; 28:672–679. [PubMed: 28843041]

7). Sheline YI, Mittler BL, Mintun MA. The hippocampus and depression. Eur Psychiatry. 2002;17:300–5.

8). Mak E, Gabel S, Su L, Williams GB, Arnold R, Passamonti L et al. Multi-modal MRI investigation of volumetric and microstructural changes in the hippocampus and its subfields in mild cognitive impairment, Alzheimer's disease, and dementia with Lewy bodies. Int Psychogeriatr. 2017; 29:545–555. [PubMed: 28088928]

9). Haukvik UK, Tamnes CK, Söderman E, Agartz I. Neuroimaging hippocampal subfields in schizophrenia and bipolar disorder: A systematic review and meta-analysis. J Psychiatr Res. 2018; 104:217–226. [PubMed: 30107268]

10). Hitti FL, Siegelbaum SA. The hippocampal CA2 region is essential for social memory. Nature 2014; 508: 88–92. [PubMed: 24572357]

11). Stevenson EL, Caldwell HK. Lesions to the CA2 region of the hippocampus impair social memory in mice. Eur J Neurosci 2014; 40:3294–3301. [PubMed: 25131412]

12). Smith AS, Williams Avram SK, Cymerblit-Sabba A, Song J, Young WS. Targeted activation of the hippocampal CA2 area strongly enhances social memory. Mol Psychiatry 2016; 21:1137–1144. [PubMed: 26728562]

13). Meira T, Leroy F, Buss EW, Oliva A, Park J, Siegelbaum SA. A hippocampal circuit linking dorsal CA2 to ventral CA1 critical for social memory dynamics. Nat Commun 2018; 9:4163. [PubMed: 30301899]

14). Monteiro BMM, Moreira FA, Massensini AR, Moraes MFD, Pereira GS. Enriched environment increases neurogenesis and improves social memory persistence in socially isolated adult mice. Hippocampus 2014; 24:239–248. [PubMed: 24123782]

15). Garrett L, Zhang J, Zimprich A, Niedermeier KM, Fuchs H, Gailus-Durner V, et al. Conditional reduction of adult born doublecortin-positive neurons reversibly impairs selective behaviors. Front Behav Neurosci 2015; 9:302. [PubMed: 26617501]

16). Pereira-Caixeta AR, Guarnieri LO, Pena RR, Dias TL, Pereira GS. Neurogenesis inhibition prevents enriched environment to prolong and strengthen social recognition memory, but not to increase BdNF expression. Mol Neurobiol 2017; 54:3309–3316. [PubMed: 27165290]

17). Pereira-Caixeta AR, Guarnieri LO, Medeiros DC, Mendes EMAM, Ladeira LCD, Pereira MT, Moraes MFD, Pereira GS. Inhibiting constitutive neurogenesis compromises long-term social recognition memory. Neurobiol Learn Mem 2018; 155:92–103. [PubMed: 29964163]

18). Cope EC, Waters RC, Diethorn EJ, Pagliai KA, Dias CG, Tsuda M et al. (2020) Adult-born neurons in the hippocampus are essential for social memory maintenance. eNeuro 2020;7:ENEURO.0182–20.2020.

19). Llorens-Martín M, Jurado-Arjona J, Avila J, Hernández F. Novel connection between newborn granule neurons and the hippocampal CA2 field. Exp Neurol 2015; 263:285–292. [PubMed: 25446721]

20). Lensjø KK, Lepperød ME, Dick G, Hafting T, Fyhn M. Removal of perineuronal nets unlocks juvenile plasticity through network mechanisms of decreased inhibition and increased gamma activity. J Neurosci 2017; 37:1269–1283. [PubMed: 28039374]

21). Pantazopoulos H, Berretta S. In sickness and in health: perineuronal nets and synaptic plasticity in psychiatric disorders. Neural Plast 2016; 2016:9847696.

22). Sorg BA, Berretta S, Blacktop JM, Fawcett JW, Kitagawa H, Kwok JCF et al. Casting a wide net: role of perineuronal nets in neural plasticity. J Neurosci 2016; 36:11459–11468. [PubMed: 27911749]

23). Yamada J, Ohgomori T, Jinno S. Perineuronal nets affect parvalbumin expression in GABAergic neurons of the mouse hippocampus. Eur J Neurosci 2015; 41:368–378. [PubMed: 25411016]

24). Carstens KE, Phillips ML, Pozzo-Miller L, Weinberg RJ, Dudek SM. Perineuronal nets suppress plasticity of excitatory synapses on CA2 pyramidal neurons. J Neurosci 2016; 36:6312–6320. [PubMed: 27277807]

25). Domínguez S, Rey CC, Therreau L, Fanton A, Massotte D, Verret L et al. Maturation of pnn and ERBb4 signaling in area CA2 during adolescence underlies the emergence of pv interneuron plasticity and social memory. Cell Rep 2019; 29:1099–1112.e4.

26). Baig S, Wilcock GK, Love S. Loss of perineuronal net N-acetylgalactosamine in Alzheimer's disease. Acta Neuropathol. 2005 110:393–401. [PubMed: 16133543]

27). Yang M, Abrams DN, Zhang JY, Weber MD, Katz AM, Clarke AM et al. Low sociability in BTBR T tf/J mice is independent of partner strain. Physiol Behav 2012; 107:649–662. [PubMed: 22245067]

28). Moy SS, Nadler JJ, Young NB, Perez A, Holloway LP, Barbaro RP et al. Mouse behavioral tasks relevant to autism: phenotypes of 10 inbred strains. Behav Brain Res 2007; 176:4–20. [PubMed: 16971002]

29). Dityatev A, Rusakov DA. Molecular signals of plasticity at the tetrapartite synapse. Curr Opin Neurobiol 2011; 21:353–359. [PubMed: 21277196]

30). York EM, Bernier LP, MacVicar BA. Microglial modulation of neuronal activity in the healthy brain. Dev Neurobiol. 2018; 78 :593–603. [PubMed: 29271125]

31). Cope EC, Gould E. Adult neurogenesis, glia, and the extracellular matrix. Cell Stem Cell 2019; 24:690–705. [PubMed: 31051133]

32). Torres L, Danver J, Ji K, Miyauchi JT, Chen D, Anderson ME, West BL, Robinson JK, Tsirka SE. Dynamic microglial modulation of spatial learning and social behavior. Brain Behav Immun 2016; 55:6–16. [PubMed: 26348580]

33). Cope EC, LaMarca EA, Monari PK, Olson LB, Martinez S, Zych AD, Katchur NJ, Gould E. Microglia Play an Active Role in Obesity-Associated Cognitive Decline. J Neurosci 2018; 38: 8889–8904. [PubMed: 30201764]

34). McFarlane HG, Kusek GK, Yang M, Phoenix JL, Bolivar VJ, Crawley JN. Autism-like behavioral phenotypes in BTBR T+tf/J mice. Genes Brain Behav 2008; 7:152–163. [PubMed: 17559418]

35). Eichenbaum H On the Integration of Space, Time, and Memory. Neuron 2017; 95:1007–1018. [PubMed: 28858612]

36). Seese RR, Maske AR, Lynch G, Gall CM. Long-term memory deficits are associated with elevated synaptic ERK1/2 activation and reversed by mGluR5 antagonism in an animal model of autism. Neuropsychopharmacology 2014; 39:1664–1673. [PubMed: 24448645]

37). Kohara K, Pignatelli M, Rivest AJ, Jung H-Y, Kitamura T, Suh J, Frank D, Kajikawa K, Mise N, Obata Y, Wickersham IR, Tonegawa S. Cell type-specific genetic and optogenetic tools reveal hippocampal CA2 circuits. Nat Neurosci 2014;17:269–279. [PubMed: 24336151]

38). Stephenson DT, O'Neill SM, Narayan S, Tiwari A, Arnold E, Samaroo HD, et al. Histopathologic characterization of the BTBR mouse model of autistic-like behavior reveals selective changes in neurodevelopmental proteins and adult hippocampal neurogenesis. Mol Autism 2011; 2:7. [PubMed: 21575186]

39). Tervo DGR, Hwang B-Y, Viswanathan S, Gaj T, Lavzin M, Ritola KD, et al. A designer AAV variant permits efficient retrograde access to projection neurons. Neuron 2016; 92:372–382. [PubMed: 27720486]

40). Lein ES, Callaway EM, Albright TD, Gage FH. Redefining the boundaries of the hippocampal CA2 subfield in the mouse using gene expression and 3-dimensional reconstruction. J Comp Neurol. 2005; 485:1–10. [PubMed: 15776443]

41). San Antonio A, Liban K, Ikrar T, Tsyganovskiy E, Xu X. Distinct physiological and developmental properties of hippocampal CA2 subfield revealed by using anti-Purkinje cell protein 4 (PCP4) immunostaining. J Comp Neurol 2014; 522:1333–1354. [PubMed: 24166578]

42). Paolicelli RC, Bolasco G, Pagani F, Maggi L, Scianni M, Panzanelli P, et al. Synaptic pruning by microglia is necessary for normal brain development. Science 2011; 333:1456–1458. [PubMed: 21778362]

43). Schafer DP, Lehrman EK, Kautzman AG, Koyama R, Mardinly AR, Yamasaki R, et al. Microglia sculpt postnatal neural circuits in an activity and complement-dependent manner. Neuron 2012; 74:691–705. [PubMed: 22632727]

44). Chung W-S, Clarke LE, Wang GX, Stafford BK, Sher A, Chakraborty C et al. Astrocytes mediate synapse elimination through MEGF10 and MERTK pathways. Nature 2013; 504:394–400. [PubMed: 24270812]

45). Harada K, Kamiya T, Tsuboi T. Gliotransmitter release from astrocytes: functional, developmental, and pathological implications in the brain. Front Neurosci 2015; 9:499. [PubMed: 26793048]

46). Beurdeley M, Spatazza J, Lee HHC, Sugiyama S, Bernard C, Di Nardo AA, et al. (2012) Otx2 binding to perineuronal nets persistently regulates plasticity in the mature visual cortex. J Neurosci 2012; 32:9429–9437. [PubMed: 22764251]

47). Spatazza J, Lee HHC, Di Nardo AA, Tibaldi L, Joliot A, Hensch TK et al. Choroid-plexus-derived Otx2 homeoprotein constrains adult cortical plasticity. Cell Rep 2013; 3:1815–1823. [PubMed: 23770240]

48). Dudek SM, Alexander GM, Farris S. Rediscovering area CA2: unique properties and functions. Nat Rev Neurosci. 2016; 17:89–102. [PubMed: 26806628]

49). Carstens KE, Dudek SM. Regulation of synaptic plasticity in hippocampal area CA2. Curr Opin Neurobiol. 2019; 54:194–199. [PubMed: 30120016]

50). McCann KE, Lustberg DJ, Shaughnessy EK, Carstens KE, Farris S, Alexander GM et al. Novel role for mineralocorticoid receptors in control of a neuronal phenotype. Mol Psychiatry. 2019; 19:10.1038/s41380-019-0598-7.

51). Hayani H, Song I, Dityatev A. Increased excitability and reduced excitatory synaptic input into fast-spiking CA2 interneurons after enzymatic attenuation of extracellular matrix. Front Cell Neurosci. 2018; 12:149. [PubMed: 29899690]

52). Hylin MJ, Orsi SA, Moore AN, Dash PK. Disruption of the perineuronal net in the hippocampus or medial prefrontal cortex impairs fear conditioning. Learn Mem. 2013; 20:267–73. [PubMed: 23592037]

53). Lee HHC, Bernard C, Ye Z, Acampora D, Simeone A, Prochiantz A, et al. Genetic OTX2 mis-localization delays critical period plasticity across brain regions. Mol Psychiatry. 2017; 22:680–688. [PubMed: 28194008]

54). Foscarin S, Raha-Chowdhury R, Fawcett JW, Kwok JCF. Brain ageing changes proteoglycan sulfation, rendering perineuronal nets more inhibitory. Aging 2017; 9:1607–1622. [PubMed: 28657900]

55). Yang S, Sylvain G, Molinaro A, Naito-Matsui Y, Hilton S, Foscarin S et al. Restoring the pattern of proteoglycan sulphation in perineuronal nets corrects age-related memory loss. bioRxiv 2020; 10.1101/2020.01.03.894188

56). Miyata S, Kitagawa H. Chondroitin 6-sulfation regulates perineuronal net formation by controlling the stability of aggrecan. Neural Plast. 2016; 2016:1305801.

57). Yang S, Cacquevel M, Saksida LM, Bussey TJ, Schneider BL, Aebischer P et al. Perineuronal net digestion with chondroitinase restores memory in mice with tau pathology. Exp Neurol. 2015; 265:48–58. [PubMed: 25483398]

58). Chafai M, Corbani M, Guillon G, Desarménien MG. Vasopressin inhibits LTP in the CA2 mouse hippocampal area. PLoS One. 2012; 7:e49708.

59). Carstens KE, Lustberg DJ, Shaughnessy EK, McCann KE, Alexander GM, Dudek SM MECP2 deletion prematurely restricts a novel window of hippocampal synaptic plasticity Soc Neurosci 2019 (abstract 187.07)

60). Sun ZY, Bozzelli PL, Caccavano A, Allen M, Balmuth J, Vicini S, Wu JY et al. Disruption of perineuronal nets increases the frequency of sharp wave ripple events. Hippocampus. 2018; 28:42–52. [PubMed: 28921856]

61). Joo HR, Frank LM. The hippocampal sharp wave-ripple in memory retrieval for immediate use and consolidation. Nat Rev Neurosci. 2018; 19:744–757. [PubMed: 30356103]

62). Okuyama T, Kitamura T, Roy DS, Itohara S, Tonegawa S. Ventral CA1 neurons store social memory. Science. 2016; 353:1536–1541. [PubMed: 27708103]

63). Daimon CM, Jasien JM, Wood WH 3rd, Zhang Y, Becker KG, Silverman JL, Crawley JN, Martin B, Maudsley S. Hippocampal transcriptomic and proteomic alterations in the BTBR mouse model of autism spectrum disorder. Front Physiol. 2015; 6:324. [PubMed: 26635614]

64). Provenzano G, Corradi Z, Monsorno K, Fedrizzi T, Ricceri L, Scattoni ML, Bozzi Y. Comparative gene expression analysis of two mouse models of autism: transcriptome profiling of the BTBR and En2 (−/−) hippocampus. Front Neurosci. 2016; 10: 396. [PubMed: 27610074]

65). Meyza KZ, Blanchard DC. The BTBR mouse model of idiopathic autism - Current view on mechanisms. Neurosci Biobehav Rev. 2017; 76:99–110. [PubMed: 28167097]

66). del Zoppo GJ, Frankowski H, Gu Y-H, Osada T, Kanazawa M, Milner R, Wang X, Hosomi N, Mabuchi T, Koziol JA. Microglial cell activation is a source of metalloproteinase generation during hemorrhagic transformation. J Cereb Blood Flow Metab 2012; 32:919–932. [PubMed: 22354151]

67). Zhang Z, Zhang Z, Lu H, Yang Q, Wu H, Wang J. Microglial polarization and inflammatory mediators after intracerebral hemorrhage. Mol Neurobiol 2017; 54:1874–1886. [PubMed: 26894396]

68). Pantazopoulos H, Gisabella B, Rexrode L, Benefield D, Yildiz E, Seltzer P, Valeri J, Chelini G, Reich A, Ardelt M, Berretta S. Circadian rhythms of perineuronal net composition. eNeuro. 2020;7:ENEURO.0034–19.2020.

69). Nguyen PT, Dorman LC, Pan S, Vainchtein ID, Han RT, Nakao-Inoue H, Taloma SE, Barron JJ, Molofsky AB, Kheirbek MA, Molofsky AV. Microglial remodeling of the extracellular matrix promotes synapse plasticity. Cell 2020; 182:388–403.e15. [PubMed: 32615087]

70). Jones-Davis DM, Yang M, Rider E, Osbun NC, da Gente GJ, Li J, Katz AM, Weber MD, Sen S, Crawley J, Sherr EH. Quantitative trait loci for interhemispheric commissure development and social behaviors in the BTBR T^{+} tf/J mouse model of autism. PLoS One. 2013; 8:e61829.

71). Wang M, He J, Zhou Y, Lv N, Zhao M, Wei H, Li R. Integrated analysis of miRNA and mRNA expression profiles in the brains of BTBR mice. Int J Dev Neurosci. 2020; 80:221–233. [PubMed: 32086829]

72). Blanchard DC, Defensor EB, Meyza KZ, Pobbe RL, Pearson BL, Bolivar VJ, Blanchard RJ. BTBR T+tf/J mice: autism-relevant behaviors and reduced fractone-associated heparan sulfate. Neurosci Biobehav Rev. 2012; 36:285–96. [PubMed: 21741402]

73). Lang BT, Cregg JM, DePaul MA, Tran AP, Xu K, Dyck SM, Madalena KM, Brown BP, Weng YL, Li S, Karimi-Abdolrezaee S, Busch SA, Shen Y, Silver J. Modulation of the proteoglycan receptor PTPσ promotes recovery after spinal cord injury. Nature. 2015; 518:404–8. [PubMed: 25470046]

74). Pendleton JC, Shamblott MJ, Gary DS, Belegu V, Hurtado A, Malone ML, McDonald JW. Chondroitin sulfate proteoglycans inhibit oligodendrocyte myelination through PTPσ. Exp Neurol. 2013; 247:113–21. [PubMed: 23588220]

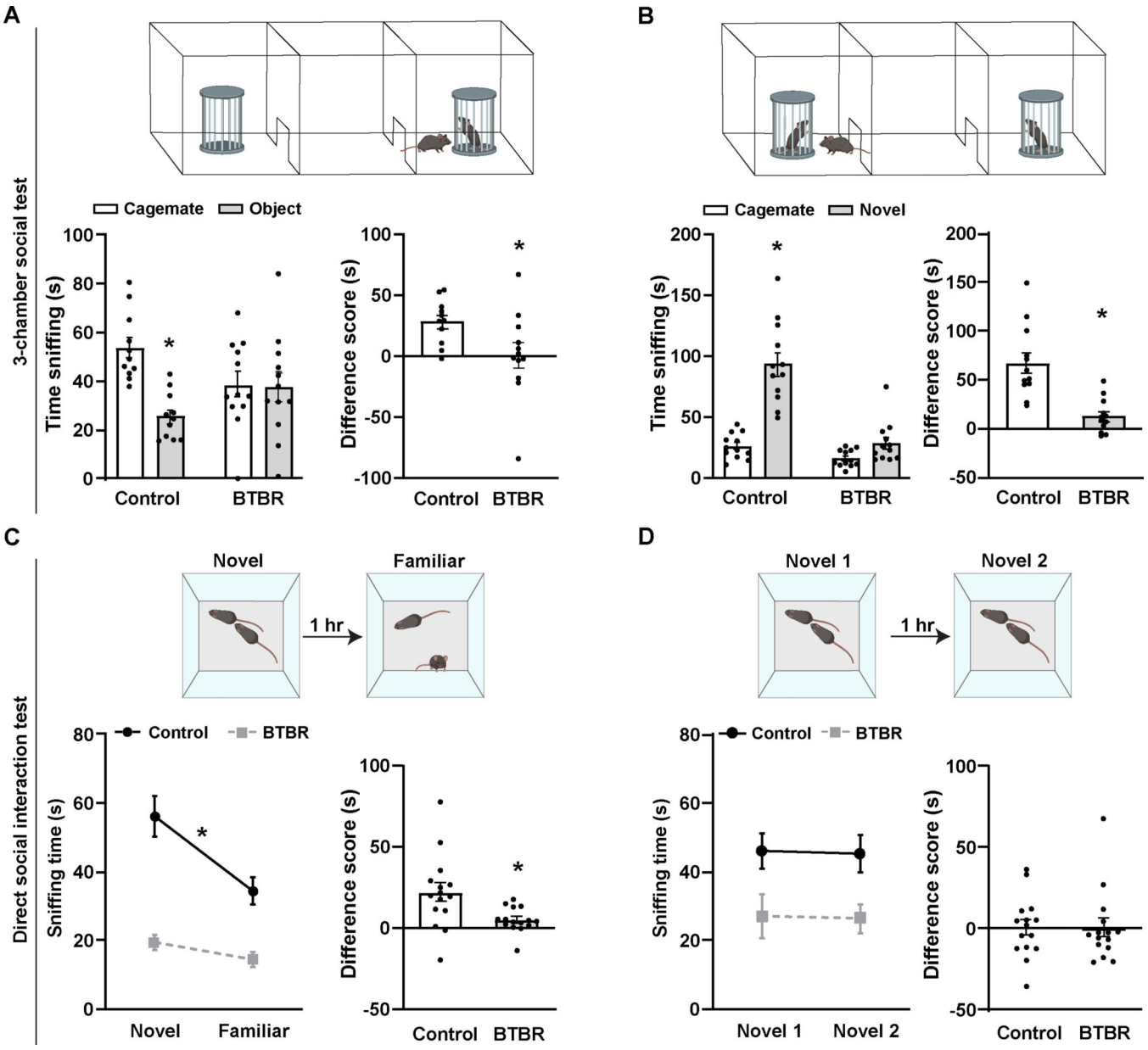

Figure 1. BTBR mice have impairments in sociability and social memory.

A. Left: Control mice display a preference for a social over nonsocial stimulus while BTBR mice show no such preference in the 3-chamber test. Control mice spent more time investigating a cagemate than a novel object and BTBR mice spent equal times investigating both stimuli (two-way ANOVA, strain: $F_{(1,42)} = 0.1097$, $p = 0.7422$, chamber: $F_{(1,42)} = 9.106$, $p = 0.0043$, strain X chamber: $F_{(1,42)} = 7.756$, $p = 0.0080$). *$p < 0.05$ compared to cagemate. Right: BTBR mice have lower difference scores (cagemate – object) compared to controls (unpaired t-test, $t_{21} = 2.25$, $p = 0.035$). $n = 11$ for controls and $n = 12$ for BTBR. *$p < 0.05$ compared to controls. **B.** Left: Control mice display robust social memory while BTBR mice exhibit no evidence of social memory in the 3-chamber social novelty test (two-way ANOVA, strain: $F_{(1,44)} = 42.50$, $p < 0.0001$, chamber: $F_{(1,44)} = 48.86$, $p <$

0.0001, strain X chamber: $F_{(1,44)} = 22.86$, $p < 0.0001$). *$p < 0.05$ compared to novel. Right: BTBR mice have lower difference scores (novel – cagemate) compared to controls (unpaired t-test, $t_{22} = 4.62$, $p = 0.00013$). $n = 12$ for both groups. *$p < 0.05$ compared to controls. **C.** Left: Control mice show evidence of social memory while BTBR mice display no such evidence in the novel to familiar direct social interaction test (two-way repeated measures ANOVA, trial: $F_{(1,28)} = 18.56$, $p = 0.0002$, strain: $F_{(1,28)} = 37.70$, $p < 0.0001$, trial X strain: $F_{(1,28)} = 7.29$, $p = 0.012$). *$p < 0.05$ control novel to familiar. Right: BTBR mice have lower difference scores (novel – familiar) compared to controls (Mann-Whitney test, $U_{28} = 49$, $p = 0.0075$). *$p < 0.05$ compared to controls. **D.** Left: Neither control nor BTBR mice decrease their investigation times for a new, novel mouse in the novel to novel direct social interaction test (two-way repeated measures ANOVA, trial: $F_{(1,28)} = 0.0398$, p = 0.8433, strain: $F_{(1,28)} = 8.443$, p = 0.0071, trial X strain: $F_{(1,28)} = 0.000746$, p = 0.9784). Right: There was no change between groups in difference scores (novel 1 – novel 2) (unpaired t-test, $t_{28} = 0.02732$, $p = 0.9784$). *$p < 0.05$ compared to controls. For panels **C** and **D**, $n = 15$ for both groups. Error bars represent SEM. See Supplementary Table 2 for complete statistics.

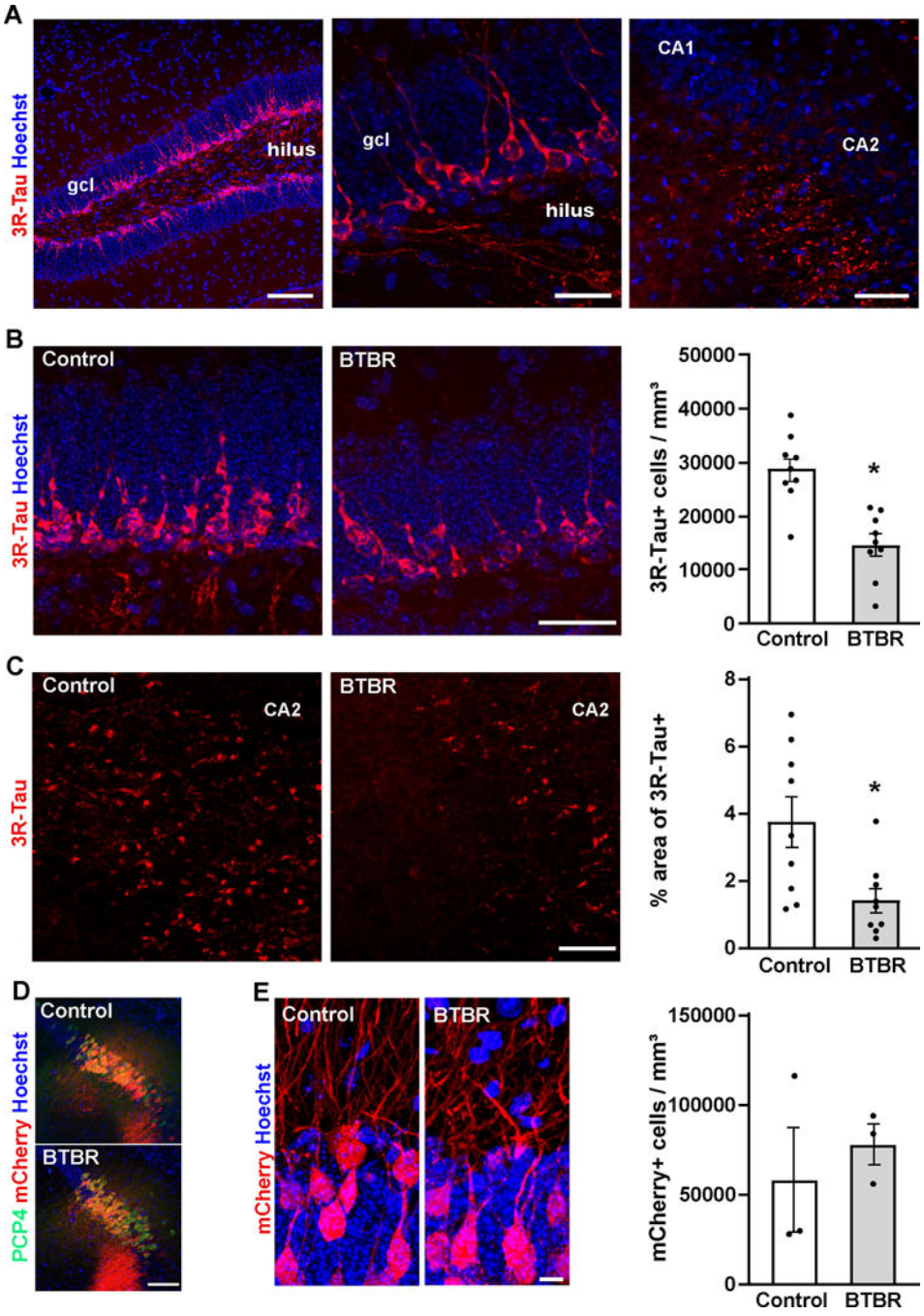

Figure 2. BTBR mice have fewer mossy fibers from abGCs to the CA2.

A. Image of the dorsal DG immunolabeled with new neuron marker 3R-Tau (red) and counterstained with Hoechst (blue) in a control mouse (left). Scale bar = 100 μm. Dorsal DG labeled with 3R-Tau+ abGCs and their mossy fiber projections in a control (middle). Scale bar = 25 μm. 3R-Tau+ mossy fiber labeling in the CA2 of a control (right). Scale bar = 50 μm. **B.** Dorsal DG immunolabeled with abGC marker 3R-Tau (red) and counterstained with Hoechst (blue) in control and BTBR mice (left). Scale bar = 25 μm. BTBR mice have fewer 3R-Tau+ abGCs in the dorsal DG compared to controls (unpaired t-test, $t_{16} = 4.73$,

$p = 0.00023$) (right). **C.** The CA2 labeled with 3R-Tau+ fibers (red) in control and BTBR mice (left). Scale bar = 50 μm. BTBR mice have less 3R-Tau+ in the CA2 (Mann-Whitney test, $U_{16} = 14$, $p = 0.019$) (right). For panels **B** and **C**, $n = 9$ for each group. **D.** CA2 of control and BTBR injected with AAV2-retro (mCherry, red) into the CA2 (PCP4, red). Scale bar = 100 μm. **E.** The DG of control and BTBR showing mCherry+ labeled granule cells after injection with AAV2-retro in the CA2. Scale bar = 10 μm. Similar expression of mCherry+ was observed in granule cells of control and BTBR mice, with no significant differences detected in the density of mCherry+ granule cells divided by the volume of the CA2 injection site (Mann-Whitney test, $U_6 = 3$, $p = 0.700$) (right). Error bars represent SEM. *$p < 0.05$ compared to controls.

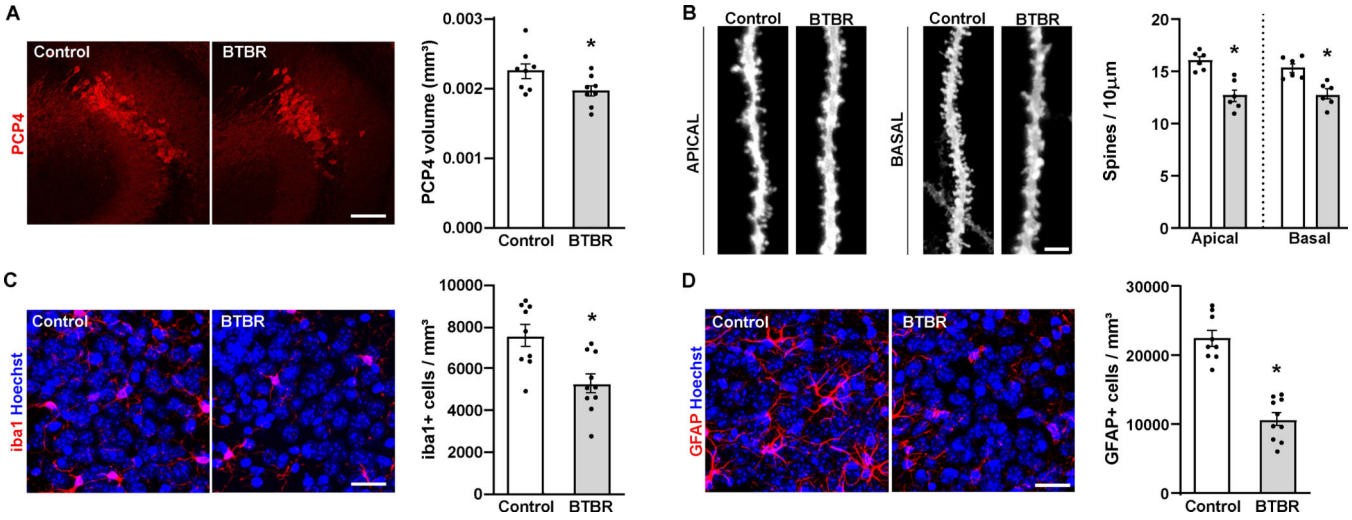

Figure 3. BTBR mice have a smaller CA2 region as well as fewer pyramidal cell dendritic spines, microglia, and astrocytes.

A. Images of the CA2 from control and BTBR mice immunolabeled with the CA2 marker PCP4 (red) (left). Scale bar = 100 µm. BTBR mice have a smaller CA2 compared to controls (unpaired t-test, $t_{14} = 2.22$, $p = 0.043$) (right). $n = 8$ for each group. **B.** Apical and basal dendritic segments from CA2 pyramidal neurons labeled with DiI in control and BTBR mice (left). Scale bar = 2.5 µm. BTBR mice have reduced dendritic spine density on apical and basal dendrites of CA2 neurons (linear mixed effects model, apical: $t_{45} = -5.088$, $p = 0.0002$, basal: $t_{43} = 3.355$, $p = 0.0017$) (right). $n = 6$ for each group. **C.** Microglia labeled with iba1 (red) in the CA2 of control and BTBR mice (left). BTBR mice have a lower density of iba1+ microglia in the CA2 compared to controls (unpaired t-test, $t_{17} = 3.40$, $p = 0.0034$) (right). **D.** Astrocytes labeled with GFAP (red) in the CA2 of control and BTBR mice (left). BTBR mice have lower density of GFAP+ astrocytes in the CA2 compared to controls (unpaired t-test, $t_{17} = 8.068$, $p < 0.0001$) (right). For panels **C** and **D**, $n = 9$ for controls and $n = 10$ for BTBR. Scale bars = 25 µm. Error bars represent SEM. *$p < 0.05$ compared to controls.

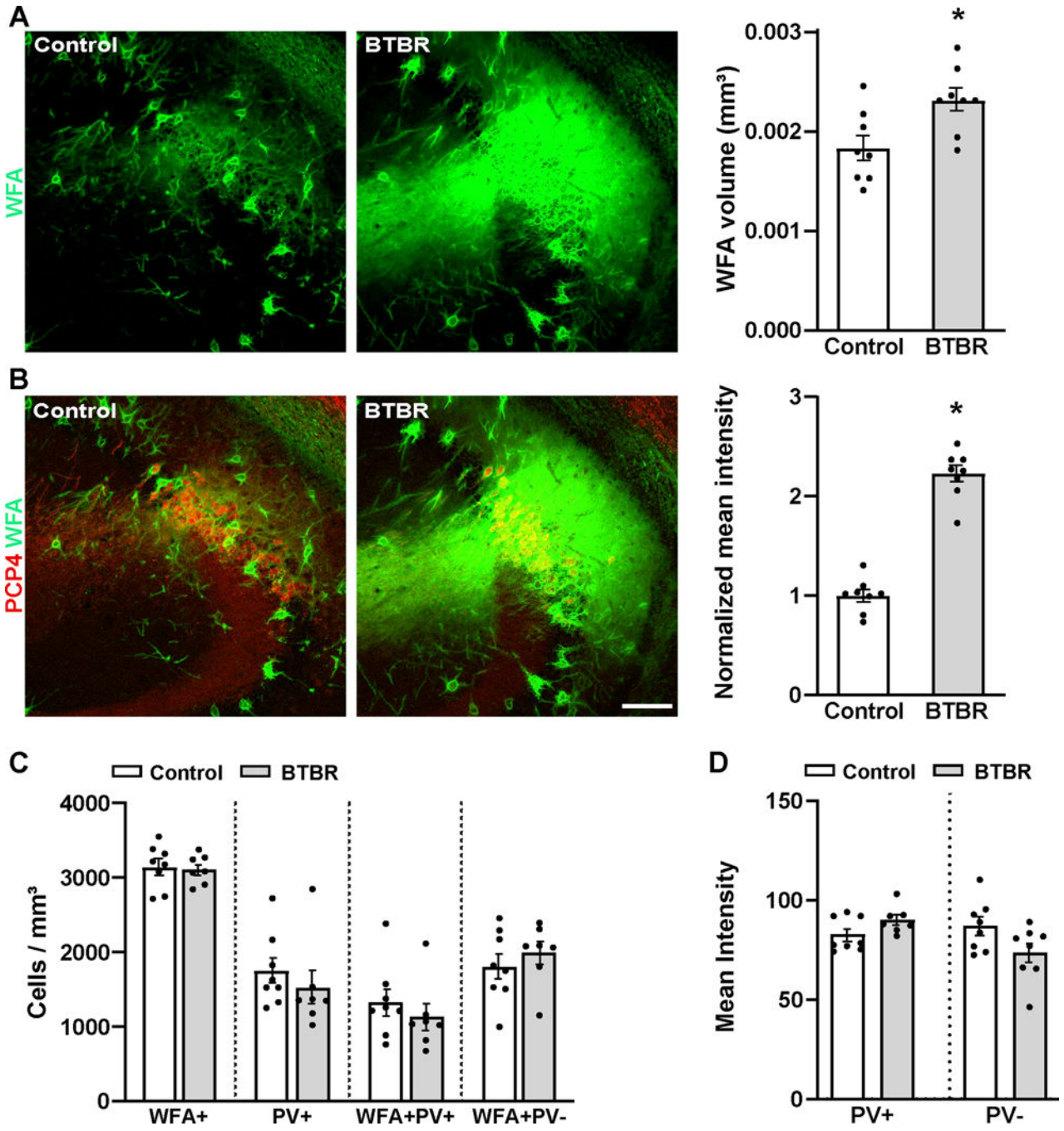

Figure 4. BTBR mice have greater WFA+ volume and intensity in the CA2 but not the vCA1.

A. Images of the CA2 labeled with the PNN marker WFA (green) in control and BTBR mice (left). BTBR mice have greater WFA+ volume in the CA2 compared to controls (unpaired t-test, t14 = 2.75, $p = 0.016$) (right). **B.** Images of PCP4 (red) and WFA (green) in the CA2 from control and BTBR mice (left). BTBR mice have increased mean intensity of WFA in the CA2 compared to controls (unpaired t-test, $t_{14} = 11.56$, $p < 0.0001$) (right). Due to the exceedingly high intensity of WFA staining in the BTBR CA2, mean intensity values were normalized to control. For panels **A** and **B**, $n = 8$ for each group. Images shown are confocal

projections made from multiple optical sections through the z plane combined to produce a single 2D image (see Supplementary Figure 2 for example optical sections demonstrating perineuronal staining of WFA in BTBR CA2). **C.** No differences in the numbers of WFA+ cells, PV+ cells, or WFA+PV+ cells were observed in the vCA1 between control and BTBR mice. **D.** No difference in WFA intensity was observed surrounding PV+ or PV- cells in the vCA1 between control and BTBR mice. For panels **C** and **D**, $n = 8$ for control and $n = 7$ for BTBR. Scale bars = 100 μm. Error bars represent SEM. *$p < 0.05$ compared to controls. See Supplementary Table 3 for complete statistics.

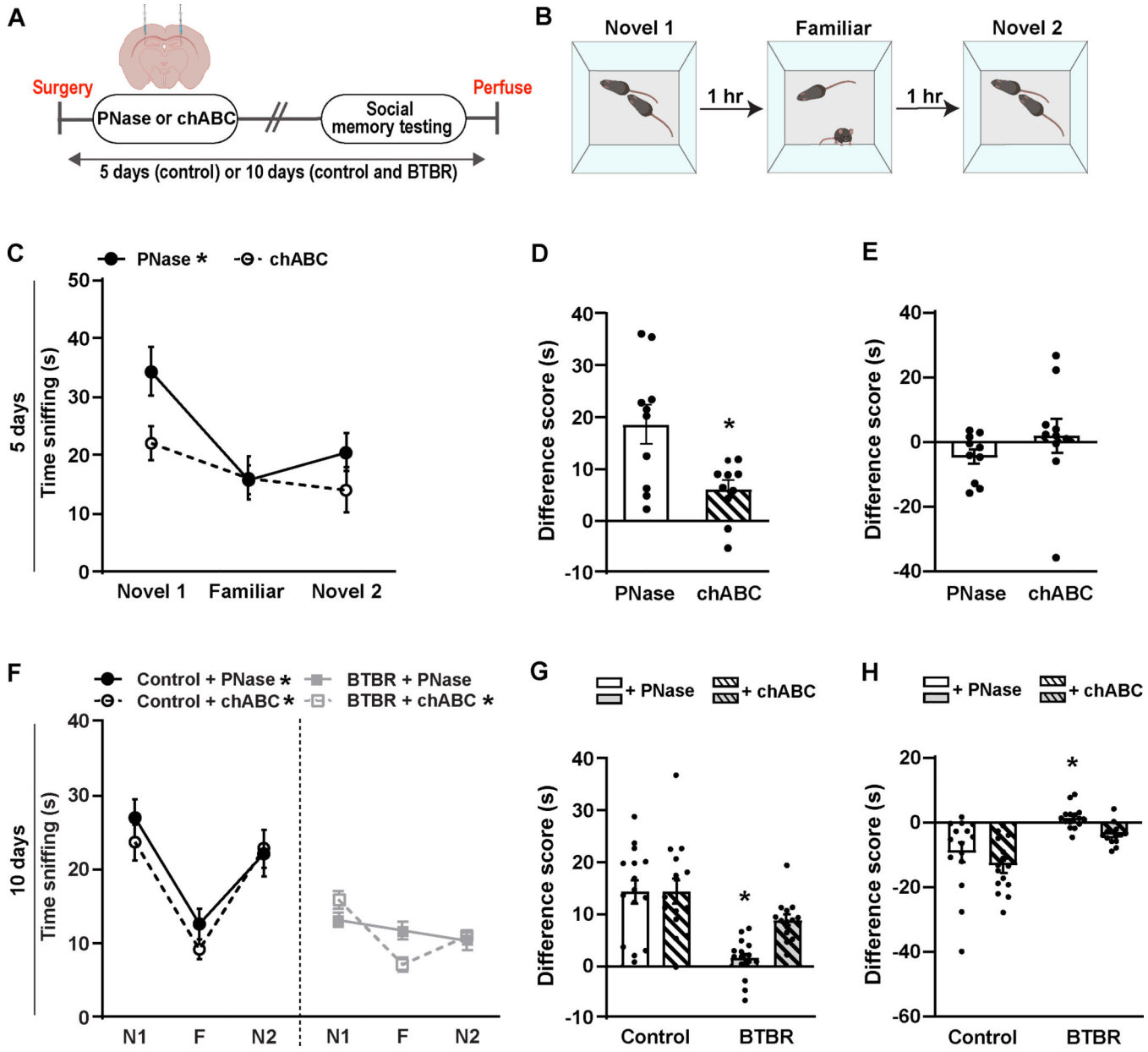

Figure 5. Reducing CA2 PNNs in control mice impairs social memory, while reducing PNNs in BTBR mice to control values partially rescues social memory impairment.

A. Timeline of experiment. Control and BTBR mice were injected with either PNase or chABC in the CA2, tested for social memory at 5 days (control mice) or 10 days (control and BTBR mice) later. **B.** Schematic of 3-trial social memory test. **C.** chABC impairs social memory (two-way repeated measures ANOVA, trial: $F_{(2,36)} = 11.90$, $p = 0.0001$; drug: $F_{(1,18)} = 2.757$, $p = 0.1142$; trial X drug: $F_{(2,36)} = 2.593$, $p = 0.0\ 87$). *$p < 0.05$ Control PNase novel 1 to familiar. **D.** chABC-treated control mice have lower difference scores (novel 1 – familiar) compared to PNase-treated mice (Mann-Whitney test, $U_{18} = 21$, $p = 0.0288$). *$p < 0.05$ compared to controls. **E.** There was no significant change between groups in difference scores (familiar – novel 2) (unpaired t-test, $t_{18} = 1.16$, $p = 0.2613$). *p

< 0.05 compared to controls. **F.** While BTBR mice treated with PNase showed no evidence of social memory, BTBR mice treated with chABC showed evidence of social memory (three-way repeated measures ANOVA, trial: $F_{(1.872,103.0)} = 48.52$, $p < 0.0001$; strain: $F_{(1,55)} = 29.46$, $p < 0.0001$; trial X strain: $F_{(2,110)} = 16.08$, $p < 0.0001$; drug: $F_{(1,55)} = 0.6334$, $p = 0.4295$; trial X drug: $F_{(2,110)} = 3.061$, $p = 0.0508$; trial X strain X drug: $F_{(2,110)} = 1.904$, $p = 0.1538$). *$p < 0.05$ from novel 1 to familiar. **G.** BTBR mice treated with chABC investigated the novel mouse more than the familiar mouse and this difference was greater than that of BTBR mice treated with Pnase (novel 1 – familiar) (two-way ANOVA, strain: $F_{(1,55)} = 26.69$, $p < 0.0001$; drug: $F_{(1,55)} = 4.365$, $p = 0.0413$; strain X drug: $F_{(1,55)} = 4.062$, $p = 0.0488$). *p <0.05 compared to all other groups. **H.** Unlike BTBR mice treated with PNase, BTBR mice treated with chABC investigated the familiar mouse more than the second novel mouse (familiar – novel 2) (two-way ANOVA, strain: $F_{(1,55)} = 27.96$, $p < 0.0001$; drug: $F_{(1,55)} = 5.756$, $p = 0.0199$, strain X drug: $F_{(1,55)} = 0.07349$, $p = 0.7873$). *p < 0.05 compared to Control + PNase and Control + chABC. For panels **C** - **E**, $n = 10$ for each group. For panels **F** - **H**, $n = 15$ for control groups, $n = 15$ for BTBR + PNase, and $n = 14$ for BTBR + chABC. Error bars represent SEM. See Supplementary Table 4 for complete statistics.